Solder joint reliability predictions using physics-informed machine learning

de Jong, S. D.M.; Ghezeljehmeidan, A. G.; van Driel, W. D.

DOI
10.1016/j.microrel.2025.115797

Publication date
2025

Document Version
Final published version

Published in
Microelectronics Reliability

Microelectronics Reliability 172 (2025) 115797

Contents lists available at ScienceDirect

Microelectronics Reliability

journal homepage: www.elsevier.com/locate/microrel

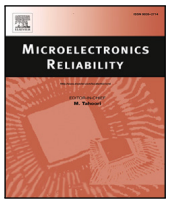

Research Paper

Solder joint reliability predictions using physics-informed machine learning

S.D.M. de Jong [a,*], A.G. Ghezeljehmeidan [a], W.D. van Driel [a,b]

[a] Department of Microelectronics, Delft University of Technology, Mekelweg 4, Delft, 2628 CD, Netherlands
[b] Signify, High Tech Campus, Eindhoven, 5656 AE, Netherlands

ARTICLE INFO

Keywords:
Solder joint reliability
Finite elements
Long short-term memory
Physics-informed neural network

ABSTRACT

The reliability of solder joints plays an increasingly important role in power electronics. The thermal fatigue experienced due to the temperature fluctuations cause catastrophic failures. However, the ability to predict the fatigue for different thermal cycles is lacking. Experimental or simulation based approaches are typically too expensive to be conducted for a wide range of thermal loading conditions. A physics informed Long Short-Term Memory (PI-LSTM) is proposed here for predicting the plastic strain and related fatigue lifetime in solder joints. The LSTM model is trained on data generated by FEM simulations, enhanced by incorporating the flow rule into the loss function. The PI-LSTM accurately predicts the plastic strain and the stress components, enabling efficient reliability predictions. Using different reliability models, the estimated cycles to failure are found to be in close agreement with those from conventional FEM simulations, demonstrating the PI-LSTM's capability for reliability assessments.

1. Introduction

The demand for reliable power electronics is increasing, from renewable energy sources such as wind and solar to electric vehicles. Many of the applications of power electronics are safety critical, e.g. aerospace, and of high strategic importance, e.g. telecommunications and power grids. The reliability and dependability of the critical components is paramount. A leading cause of failures of power electronics is due to the large amounts of heat generated during operation [1]. The thermomechanical effects caused by the temperature fluctuations are a result of the differences in the Coefficient of Thermal Expansion (CTE) and Young's modulus of the different materials present in the package. To estimate the lifetime of the component over large timescales, experimental techniques such as the Accelerated Thermal Cycling Test (ATCT) are commonly used in industry. The ATCT allows for accurate assessments of a products reliability. However, the experimental approach of the ATCT is time consuming and costly. A more efficient method is found in the use of simulation techniques such as the Finite Element Method (FEM). A simulation of the packages response to the thermal load can be determined at a reduced cost. Nevertheless, an accurate simulations requires an experienced engineer to setup the simulations, e.g. building the geometry and mesh, as well as computational resources and time for the actual simulation. Simulations are therefore used for only a few loading conditions at most.

To obtain the reliability of the package to a wider range of thermal loading conditions, a more efficient approach needs to be used. This is where the use of Artificial Intelligence (AI) shows a lot of promise, and has found its way into the field of microelectronic reliability. A lot of recent work has gone into using AI for microelectronic packaging. Popular methods include Supported Vector Regression (SVR) in [2–5] for its suitability to high dimensional features, Random Forest [3,5,6] (RF) because it is good for classification, K-Nearest Neighbors [6,7] (KNN) for its ability to handle multiclass classification, Artificial Neural Networks [8,9] (ANN) for its flexibility, Convolutional Neural Network for handling grid like data structures [10] (CNN), and Recurrent Neural Network [11] (RNN) for its ability to handle time series data. A more extensive overview of the emergence of AI in the reliability of microelectronics we refer to [12]. It is notable that the majority of the research in AI for microelectronics is focused on the design of the package, but the effect of different loading conditions is lacking. This work will therefore use AI for predicting the reliability of package with a given geometry under different thermal loads.

The downside to most of these proposed approaches is that in order to train a model large amounts of data are required. For example, the Insulated Gate Bipolar Transistor (IGBT) is characterized with Bayesian machine learning in [13] using 230 datasets. In [14] the health status of an IGBT is assessed using adaptive network-based fuzzy inference system (ANFIS) algorithm, trained with a dataset of 1257. To estimate the Remain Useful Lifetime (RUL) of solder joints [15] used an ANN trained with 8000 data points, [16] used 265, while [17] used RF with a dataset of 295. The large amount of training data required to train

* Corresponding author.
E-mail address: S.D.M.deJong@tudelft.nl (S.D.M. de Jong).

https://doi.org/10.1016/j.microrel.2025.115797
Received 19 December 2024; Received in revised form 15 April 2025; Accepted 19 May 2025
Available online 12 June 2025

these models has serious disadvantages because larger datasets tend to increase the training time, and constructing the datasets takes more effort.

To reduce the amount of data required for training the model, first a suitable method must be selected. Given the time dependent responses of the ATCT, and thus the sequentially generated data, the Long Short-Term Memory (LSTM) [18] network is a natural choice. The LSTM is a Recurrent Neural Network (RNN) designed for training on sequential data. The LSTM does not suffer from exploding or vanishing gradients common in most RNNs [19]. A typical LSTM network is composed of several layers, such as input, output, LSTM, and fully connected layers. The LSTM layer processes sequences by passing input sequences through a collection of LSTM cells and generating corresponding output sequences. Each LSTM cell has gates that manage information flow, memory updates, and output generation, making it effective for modeling sequence data. Finally fully connected layers on top, bridge LSTM output to the final predictions by generating the required output features [20].

Nevertheless, the LSTM still requires large amounts of data for training before it can make accurate predictions. This data has to come from either experiments or simulations, but that, as previously discussed, that a lot resources. In order to reduce the amount of data required for training the LSTM a Physics-Informed Neural Network (PINN) [21] is used in conjunction with the data driven LSTM. A PINN incorporates Partial Differential Equations (PDE) describing the physical system into the training process [22]. Including the PDEs in the loss function increases the robustness and accuracy of the trained model, thereby reducing the amount of necessary training data. Moreover PINNs have demonstrated remarkable generalizability across a broad spectrum of physical systems, ranging from fluid dynamics to nonlinear structures and elasto-plastic materials [21–26] highlighting their versatility in addressing both forward and inverse problems across various PDE-governed domains.

2. Methodology

To be able to create a model to predict the plastic strain in BGA packages, a number of things need to be done first. The package with its dimensions and materials need to be defined, next the necessary data has to be created in order to train the model, and lastly the machine learning algorithm needs to be set up. This section will provide all the preconditions and setups required for training the physics informed LSTM model (see Fig. 1).

2.1. Geometry, materials and loading conditions

This paper proposes a PI-LSMT trained on a small dataset, while keeping the ability to predict soldier joint fatigue with high accuracy, Therefore, the choice was made use a two dimensional FEM simulation, to reduce the computational cost of generating the dataset. The package can be approximated by a 2D geometry because the failure usually occurs in the solder joint farthest from the center [4]. The package used in this work is a multi-component package consisting of a PCB, Under Bump Metalizations (UBM), copper pads, a Stress Boundary Layer (SBL), a silicon chip and the solder balls. The dimensions of the package are provided for a two dimensional package in Table 1 in micrometers.

The solder joint is made from different materials. For this work all materials are assumed to be homogeneous and isotropic. For the solder ball the widely used SAC305 solder is used, with a temperature dependent Young's Modulus. Furthermore, the Young's modulus is non-linear, that is plasticity is considered in addition to elasticity, in accordance with the work from [27]. The other materials in the solder joint are assumed to be perfectly elastic. The properties of the materials used for each component are provided in Table 2. To examine the package resistance to thermal fatigue, the solder joints are subjected to a range of different temperature cycles. The external temperature is periodically changed between a maximum and minimum temperature, the rate at which the temperature is changed is defined by the ramp rate. Additionally, once reaching either the minimum or maximum temperature, it is kept their for a time defined by the dwell time, in order to reach a thermal equilibrium within the package. The thermal cycle used is based on the JEDEC standards, widely used in the microelectronics industry. The minimum and maximum temperatures are 233.15 K and 398.15 K respectively. Previous observations of the plastic deformation in the solder has shown that the ramp rate has the highest impact on the fatigue life. Therefore, the ramp rates are varied between 10 K/min and 15 K/min for the temperature cycles in this work.

Table 1
Dimensions of the package.

Component	Dimensions [μm]
PCB	3900 × 1000
Ball diameter	250
Cu pad	220 × 25
UBM	190 × 8.6
SBL	2000 × 15.5
Si chip	2000 × 330

Table 2
The material properties.

Material	CTE [10^{-6} 1/K]	Young's modulus [GPa]	Poisson ratio [–]
PCB	23.9	18.2	0.30
SAC305	25	Non-linear	0.35
Copper	16.7	68.9	0.34
SBL	55	2	0.33
Silicon	2.62	129	0.28

2.2. Physics informed LSTM

A Physics-Informed Long Short-Term Memory (PI-LSTM) is employed to predict the plastic deformation in the solder joint at any point in time, using only on the transient ambient temperature as an input. To normalize the data, a *tanh* layer is used to ensure stability. The temporal data, e.g. the plastic strain at each time instance, has to be available to the model in order for it to train. The training data is created using an FEM simulation to model the response of the package to the thermal cycling. To reduce the amount of training data required and to speed up the training itself, the ideas from PINN are introduced to the model. In order to make the LSTM physics informed a partial differential equation (PDE) needs to be injected into the loss function. The PDE is taken from the flow rule of plasticity. The yield function f is determined by

$$f(\sigma_{ij}, T, \varepsilon^p_{eq}) = \sigma_v(\sigma_{ij}) - \sigma^0_{ys}(T) - h(\varepsilon^p_{eq}), \tag{1}$$

where σ^0_{ys} is the temperature dependent initial yield stress, h the hardening function, and σ_v the von Mises stress calculated for the plain strain as

$$\sigma_v = \sqrt{\sigma^2_{xx} - \sigma_{xx}\sigma_{yy} + \sigma^2_{yy} + \sigma_{zz} + 3\tau^2_{xy}}, \tag{2}$$

based on the components of the stress tensor σ_{ij}. If the change to the yield function remains smaller or equal to zero, i.e. $f + df \leq 0$, no plasticity occurs, but if the increment is larger than zero, $f + df > 0$, plasticity does occur such that the recalculated value is equal to zero, i.e. $f = 0$. The plastic strain tensor is determined by the PDE for the flow rule

$$d\varepsilon_{ij} = d\lambda \frac{\partial f}{\partial \sigma_{ij}}, \tag{3}$$

where $d\lambda$ is the plastic multiplier subject to $d\lambda \geq 0$. The PDE in (3) can be used in the loss function of the LSTM network for the physics informed part of the PI-LSTM. The PI-LSTM is setup as following. The training data contains the equivalent plastic strain, stress components,

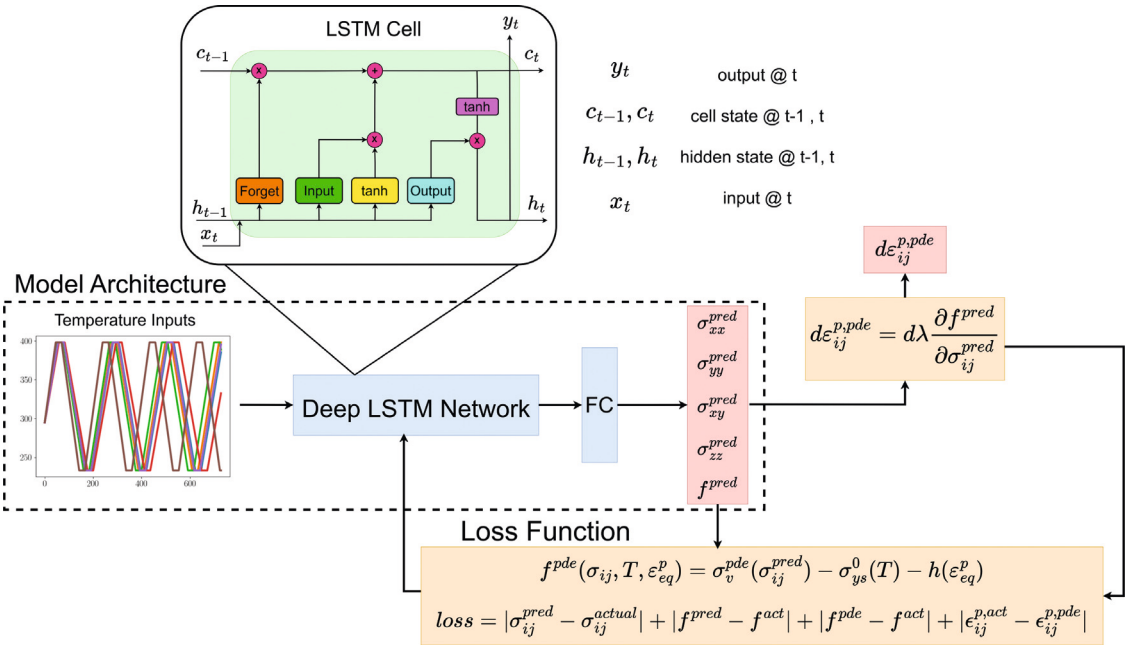

Fig. 1. Overview of the workflow of the PI-LSTM.

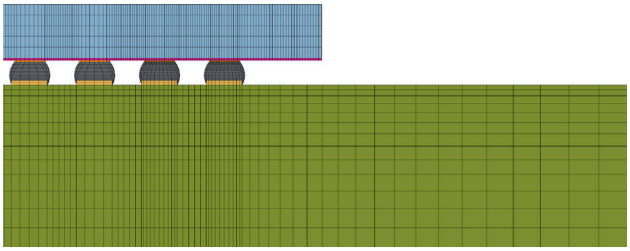

Fig. 2. The mesh used for the FEM simulations.

the ambient temperature and the current yield stress. The model outputs the individual stress components and the current yield stress, from which the flow rule can be solved. Additionally, the predicted value of the plastic multiplier $d\lambda$ is optimized by including it as a trainable parameter.

2.3. Generating data with the finite element method

To create the required training data for the PILSTM simulations are performed on the solder joint geometry from Table 1. FEM simulations have been widely used to simulate the response of solder joints to thermal conditions [28,29], it is therefore a natural choice to use here. To ensure accurate results for use as the training data the boundary conditions, the mesh quality, and the mesh dependency have to be carefully selected. The displacement at the left most boundary is restricted in horizontal direction, with the lowest point being restricted in vertical direction as well. This results in a symmetrical boundary condition in that line, reducing the computational cost of simulating the entire package by half. To discretize the domain a structured rectangular mesh has been used to ensure an acceptable mesh quality. The mesh size is refined in areas where the deformations are expected to be greatest, e.g. near the solder ball, and a courser mesh is used elsewhere to reduce the simulation time. The plastic deformation that occurs inside the solder ball is highly dependent on the shape and size of the mesh elements used. To mitigate this effect and to obtain accurate results the mesh size is deliberately chosen. As the largest plastic strain tends to occur at the top right corner of the outermost solder ball, the critical mesh size has been chosen to be 12.5 μm by 6.4 μm in accordance with [30]. The innermost solder ball have been simulated using a courser mesh to further reduce the cost of the simulation. The mesh used for all the simulations performed in this work is shown in Fig. 2.

The simulations are performed using COMSOL Multiphysics® [31], using the described discretization. The relevant data is extracted in a single point in the critical area of the outermost solder ball, that is the top right corner of the solder on the far right. A total of 66 simulations have been performed, using the temperature cycles shown in Fig. 3(a), where the extrema of the ramp rates are shown in bold. The test cases are created by randomly selecting 5 cases. The ramp rates for these cases are 11.056, 11.455, 11.887, 11.065 and 13.696 K/min, giving a good range of values. Some of the ramp rate values, mainly case 1 and case 4, are quite close. This is due to the test data being randomly selected from the available dataset. The remaining dataset is used for training the model.

Because the time dependent behavior of the solder joints requires a relatively small time step for an adequate temporal stability, the created datasets are very large, causing the training time of the model to become very time consuming due to the linear algebra operations that have the be done. In order to achieve a reasonable training time for the proposed PILSTM model, the size of the datasets is significantly reduced, by only exporting the results of every 100th time step of the simulation.

3. Predicting plastic strain and reliability

The behavior of the solder joint to the changing ambient temperature has been successfully simulated. An representative example of the simulation results is provided in Fig. 4, where the highest plastic strain does indeed occur in the critical area, as the case in other works [32,33]. This is a good indicator that the simulations performed here are able to output a physically valid result. Especially since the training data is taken exclusively from this area. Once the PILSTM was trained using the 60 training sets, the equivalent plastic strain was predicted as is shown in Fig. 5.

The predicted plastic strain is a close match to the FEM results for the first few cycles. The increases, decreases and dwell times of the ambient temperature can be clearly seen in the response of the plastic strain, the plastic strain increases when the temperature is ramping,

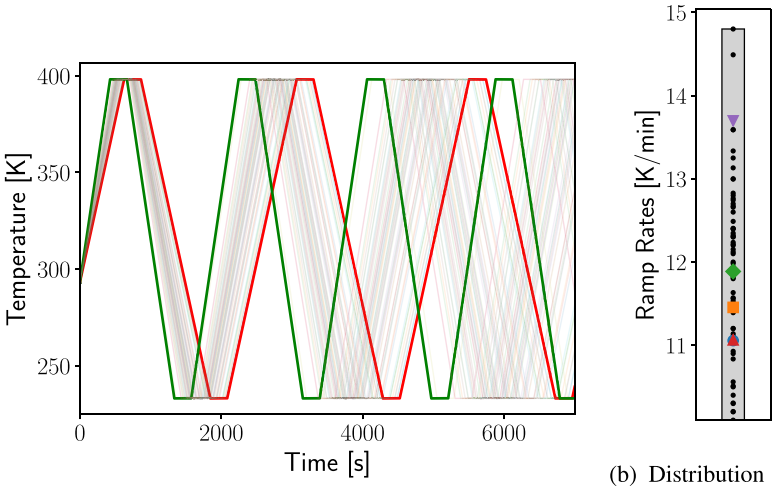

(a) The temperature cycles used for simulating. The cycles with minimum and maximum ramp rates have been plotted in bold.

(b) Distribution of the ramp rates. The test cases have been highlighted.

Fig. 3. The temperature cycles and ramp rates.

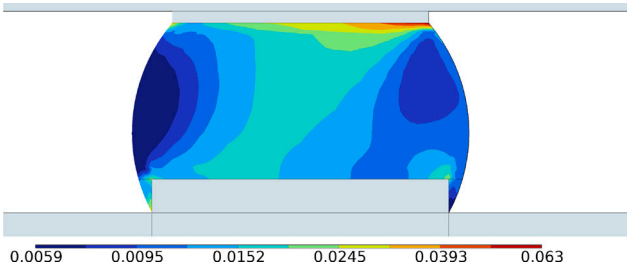

Fig. 4. The location of the maximum plastic strain in the solder joint.

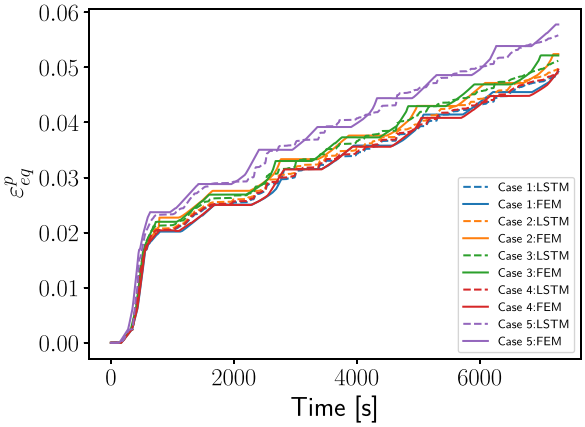

Fig. 5. The equivalent plastic strain ε^p_{eq} from FEM simulations and LSTM predictions.

but it plateaus once the ambient temperature remains constant. After about three thermal cycles the values predicted by the PILSTM are seen to be less aligned with the simulated results, i.e. the effect of the temperature changes is no longer that pronounced. Nevertheless, the predicted plastic strain continues to follow the general upwards trend of the plastic deformation, the end value of the plastic strain matches closes with the simulated value.

The improvement of the prediction time from the PI-LSTM is noteable. The FEM simulations performed on a *13th Gen Intel(R) Core(TM) i7-1365U, 1800 Mhz, 10 cores, 12 threads* with *16 GB RAM*, took around 38 min per simulation. Simulating all 66 simulations took about 41 h. This time could be improved by using more powerful computational resources, but one should note that here a 2D problem is simulated instead of a more computationally expensive 3D problem. Therefore, this is still a good indication of the time it takes to create the datasets required for training an AI model. Meanwhile, a prediction with the PI-LSTM takes but a few seconds, highlighting the efficiency of the PI-LSTM over FEM simulations.

Apart from the equivalent plastic strain, the stresses present in the critical point are also predicted by the PILSTM, the values for the non-zero stress components are shown together with the simulated values in Figs. 6–9. The predicted stresses show excellent agreement with the simulated values. The same cyclical behavior can be observed in the predicted stresses along the entire path of the simulated results. It can thus be concluded that the proposed PILSTM is able to achieve accurate stress predictions. The reason the accurate prediction of the stress components does not translate into the same performance in the plastic strain prediction is likely due to the prediction of the plastic multiplier $d\lambda$. The value of the plastic multiplier as predicted by the LSTM model is shown in Fig. 10. The predicted value is in violation of the positive plastic multiplier condition $d\lambda \geq 0$, which implies that plasticity could be reversed. However, from Fig. 5 it is observed that the plasticity never decreases, so this unphysical behavior does not actually happen. In fact, the yield function f from (1) behaves as would be expected from a cyclical problem, as is shown for the first test case in Fig. 11. The values is near zero when the equivalent plastic strain increases, and drops below zero during the dwell times.

3.1. Predicting cycles to failure

Having determined the models ability to predict the plastic strain and stress components, the applicability of the proposed model in reliability assessments is investigated further. The equivalent plastic strain can be used to estimate the number of cycles the solder joint can withstand until failure. For this estimation multiple models have been proposed throughout the years. One such model is the CALCE model [36]. The CALCE model related the cycles to failure to the equivalent plastic strain by the equation

$$N_f = \frac{1}{2}\left(\frac{\Delta\varepsilon^p_{eq}}{2\varepsilon_f}\right)^{\frac{1}{c}}, \tag{4}$$

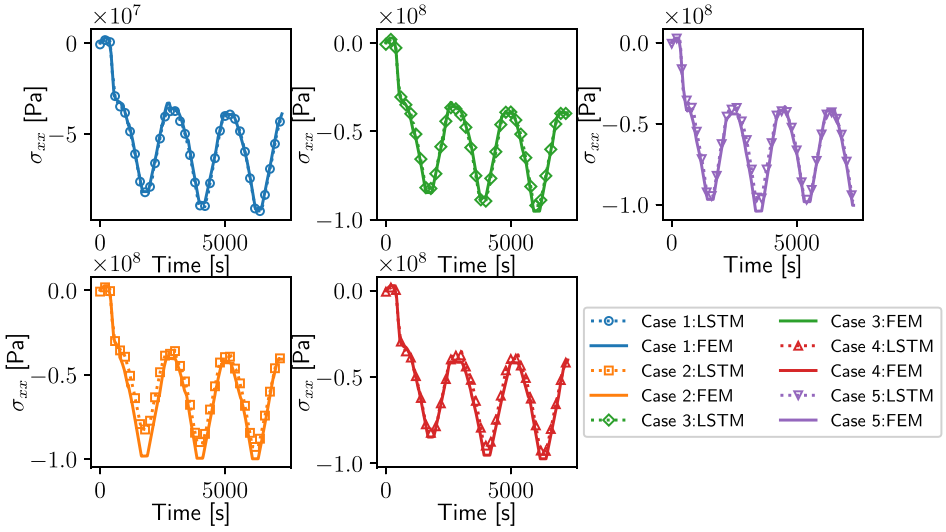

Fig. 6. Stress component in xx-direction.

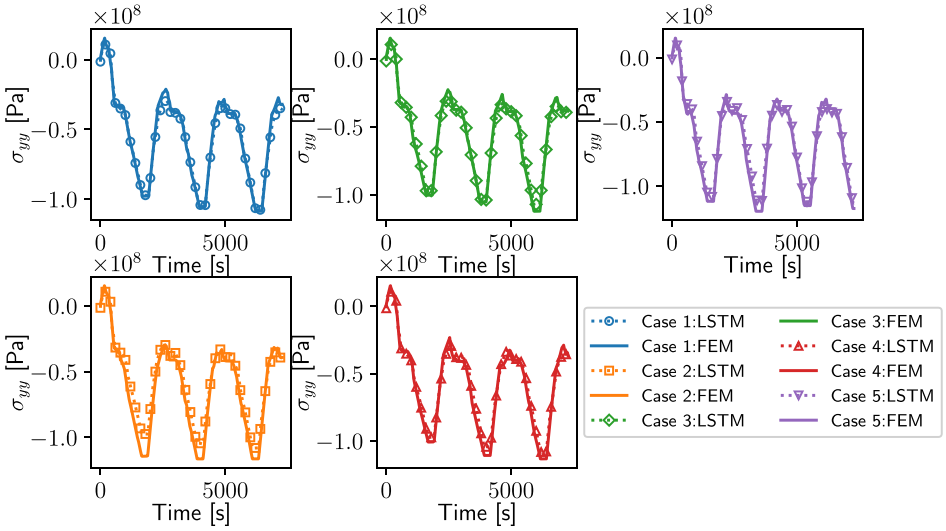

Fig. 7. Stress component in yy-direction.

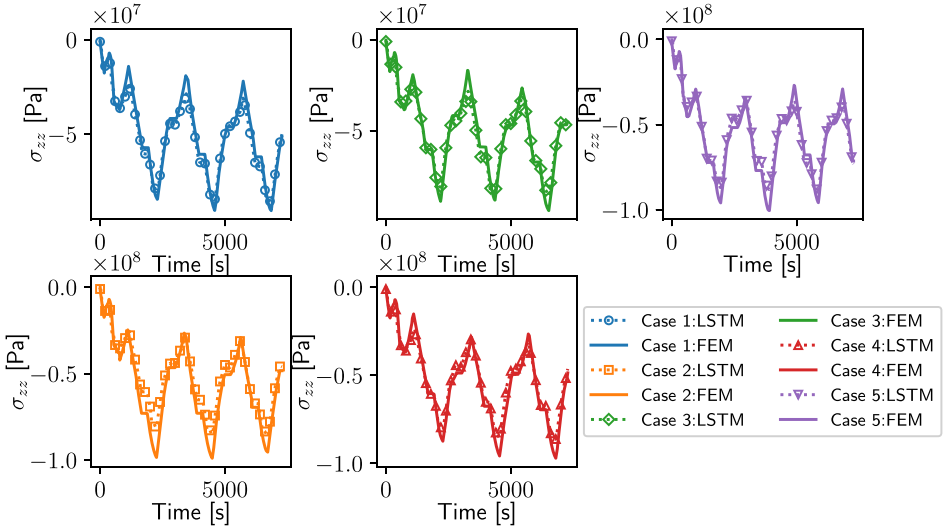

Fig. 8. Stress component in zz-direction.

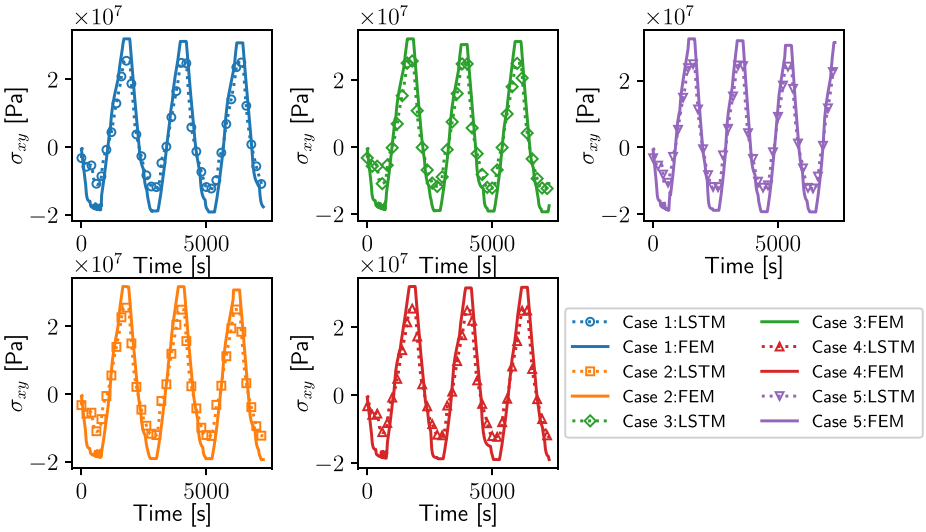

Fig. 9. Stress component in xy-direction.

Table 3
Previous ML studies compared to the PI-LSTM.

Source	Year	Method	Size of dataset	R2-score
Bhat et al. [15]	2023	MLP	8000	0.72
Quispe-Aguilar et al. [13]	2023	BML	230	0.962
Bani Hani et al. [34]	2023	ANN	189	0.94
Alavi et al. [16]	2024	DT, RF, LR, KNN, XGBoost, ANN	265	0.5458
				0.7210
				0.5824
				0.6015
				0.8454
				0.8493
Rebai et al. [17]	2025	MLR, PR, DTR, RFR, SVMR, RR, LAR, EnetR	295	0.987339
				0.996886
				0.995743
				0.997319
				0.961701
				0.978226
				0.979976
				0.983949
Qasaimeh et al. [35]	2025	ANN, LME, MLR, DT	890	0.8895
				0.9179
				0.9007
				0.7752
This work	2025	PI-LSTM	66	0.991265072

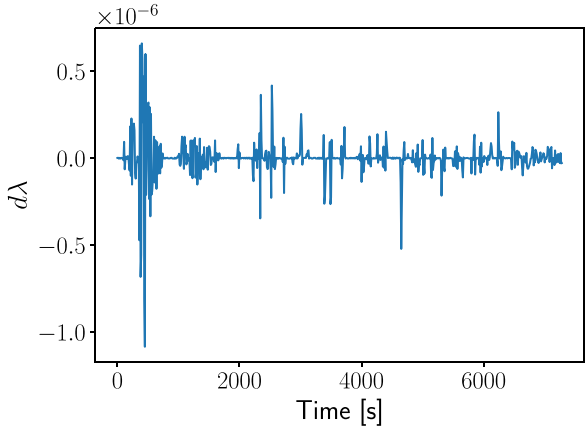

Fig. 10. The plastic multiplier $d\lambda$ for test case 1.

where ε_f is the fatigue ductility constant and c the fatigue ductility exponent. Another way to predict the number of cycles to failure comes from the work of Syed [37], in which the number of cycles is predicted by

$$N_f = \frac{1}{C\Delta\varepsilon_{eq}^p}, \tag{5}$$

where the constant C is 0.0358 for SAC solder joints. Lastly, a common method for estimating the solder joint reliability is the Coffin–Manson model. The Coffin–Manson model uses the equation

$$N_f = C(\Delta\varepsilon_{eq}^p)^{-\eta}, \tag{6}$$

where $C = 0.235$ and $\eta = 1.75$ for SAC solder joints [38]. The estimated cycles to failure for (4)–(6) are provided in Fig. 12 for all five test cases. The different equations give different values for the cycles to failure, the Coffin–Manson the lowest, Syed higher, and the CALCE is gives far higher values. The differences between the values obtain for FEM simulations and the predictions from the PI-LSTM are relatively small. The proposed LSTM model is therefore not only effective at predicting the stresses and strains in the solder joint, but can also be used for estimating the lifetime of solder joints.

To compare the proposed PI-LSTM to other methods, the R2-score is determined. The R2-score of the 5 test cases are 0.994, 0.983, 0.995,

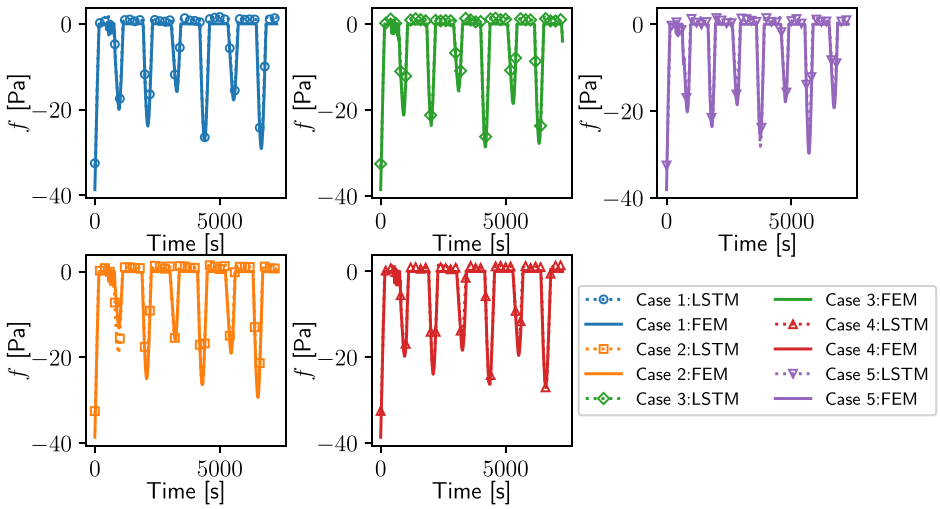

Fig. 11. The yield function f.

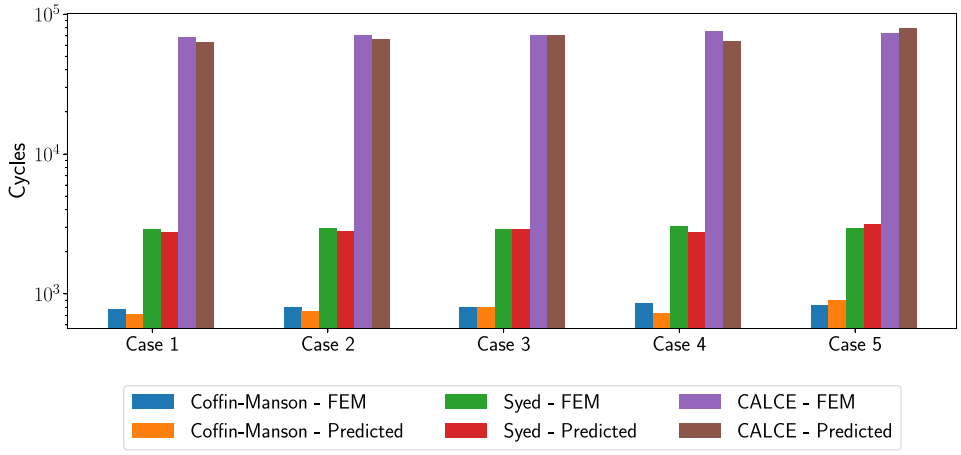

Fig. 12. Cycles to failure for different reliability models.

0.993, and 0.992 respectively. The average R2-score of the 5 test cases is 0.991. This score can be compared to other methods to determine the effectiveness of the PI-LSTM. Detailed information on recent works using ML to predict the reliability of power electronics is provided in Table 3. The table provides information on a wide range of models, the size of the dataset used to train the model, and the R2-score the model achieved. From Table 3, it can be observed that some methods are able to achieve a similarly high R2-score. However, the size of the dataset used for training is much larger than the 66 used for the proposed PI-LSTM model. This shows that the PI-LSTM is able to achieve good results in comparison to other models, while using minimal data for train the model.

4. Conclusion

This study presents a novel approach for determining the reliability of a solder joint by predicting the plastic strain. Results from FEM simulations were used to train an LSTM model augmented by the inclusion of the flow rule within its loss function. This physics informed LSTM model demonstrated high accuracy and good stability, for a relatively small amount of training data. The PI-LSTM predicts the equivalent plastic strain ϵ^p_{eq} as well as the stress components present in the solder joint. The predicted plastic strain can be used to determine the reliability by relating it to the cycles to failure. Multiple reliability models show the cycles to failure predicted by the proposed PI-LSTM are in close proximity to the results from FEM simulations,highlighting the models potential for applications in reliability assessments. When the results from the PI-LSTM are compared to other methods from literature shows it achieves similar or higher R2-scores, even though these dataset used by the PI-LSTM is much smaller. This significantly reduces the time required for creating a database for training an AI. Additionally, the proposed model can be implement where data availability is too limited for other models to achieve sufficient accuracy.

CRediT authorship contribution statement

S.D.M. de Jong: Conceptualization, Methodology, Writing – original draft. **A.G. Ghezeljehmeidan:** Conceptualization, Methodology, Writing – review & editing. **W.D. van Driel:** Supervision, Funding acquisition.

Declaration of competing interest

The authors declare that they have no known competing financial interests or personal relationships that could have appeared to influence the work reported in this paper.

Acknowledgments

This research was carried out under project number N21006 in the framework of the Partnership Program of the Material innovation institute M2i (www.m2i.nl) and the Dutch Research Council (www.nwo.nl).

This work is also supported by the project EXPLAIN, the Netherlands Enterprise Agency RVO under grant AI212001.

Data availability

Data will be made available on request.

References

[1] Huai Wang, Frede Blaabjerg, Power electronics reliability: State of the art and outlook, IEEE J. Emerg. Sel. Top. Power Electron. 9 (6) (2020) 6476–6493.

[2] Fang Liu, Zhongwei Duan, Runze Gong, Jiacheng Zhou, Zhi Wu, Nu Yan, Comparative study of machine learning method and response surface methodology in BGA solder joint parameter optimization, Solder. Surf. Mount Technol. 37 (1) (2025) 25–36.

[3] Jung-Pin Lai, Shane Lin, Vito Lin, Andrew Kang, Yu-Po Wang, Ping-Feng Pai, Predicting thermal resistance of packaging design by machine learning models, Micromachines 16 (3) (2025) 350.

[4] Hsuan-Chen Kuo, Chih-Yi Chang, Cadmus Yuan, Kuo-Ning Chiang, Wafer-level packaging solder joint reliability lifecycle prediction using SVR-based machine learning algorithm, J. Mech. 39 (2023) 183–190.

[5] Sunil Kumar Panigrahy, Yi-Chieh Tseng, Bo-Ruei Lai, Kuo-Ning Chiang, An overview of AI-assisted design-on-simulation technology for reliability life prediction of advanced packaging, Mater. 14 (18) (2021) 5342.

[6] Ching-Feng Yu, Jr-Wei Peng, Chih-Cheng Hsiao, Chin-Hung Wang, Wei-Chung Lo, Development of GUI-driven AI deep learning platform for predicting warpage behavior of fan-out wafer-level packaging, Micromachines 16 (3) (2025) 342.

[7] Tanya Thekemuriyil, Jaspera Dominique Rohner, Renato Amaral Minamisawa, Machine learning-based prediction of on-state voltage for real-time health monitoring of IGBT, Power Electron. Devices Compon. 6 (2023) 100049.

[8] Kuo-Shen Chen, Wen-Chun Wu, Data-driven stress/warpage analyses based on stoney equation for packaging applications, IEEE Trans. Device Mater. Reliab. 24 (1) (2024) 112–122.

[9] Qinghua Su, Cadmus Yuan, K.N. Chiang, Utilizing ensemble learning on small database for predicting the reliability life of wafer-level packaging, in: 2024 IEEE 26th Electronics Packaging Technology Conference, EPTC, IEEE, 2024, pp. 1248–1252.

[10] Sheng-Xiang Kao, Chen-Fu Chien, Deep learning-based positioning error fault diagnosis of wire bonding equipment and an empirical study for IC packaging, IEEE Trans. Semicond. Manuf. 36 (4) (2023) 619–628.

[11] Yanwei Dai, Jiahui Wei, Fei Qin, Recurrent neural network (RNN) and long short-term memory neural network (LSTM) based data-driven methods for identifying cohesive zone law parameters of nickel-modified carbon nanotube reinforced sintered nano-silver adhesives, Mater. Today Commun. 39 (2024) 108991.

[12] Cadmus Yuan, S.D.M. de Jong, Willem D. van Driel, AI-assisted design for reliability: Review and perspectives, in: 2024 25th International Conference on Thermal, Mechanical and Multi-Physics Simulation and Experiments in Microelectronics and Microsystems, EuroSimE, IEEE, 2024, pp. 1–12.

[13] Max-Fredi Quispe-Aguilar, Rosa Huaraca Aparco, Calixto Cañari Otero, Margoth Moreno Huamán, Yersi-Luis Huamán-Romaní, A probabilistic bayesian machine learning framework for comprehensive characterization of bond wires in IGBT modules under thermomechanical loadings, J. Electron. Mater. 53 (2) (2024) 719–732.

[14] Zeyu Duan, Ran Yao, Wei Lai, Hui Li, Cheng Yang, Yuan Min, Yannan Yuan, Wenxing Han, An IGBT device health status assessment method based on characteristics identification, IEEE Trans. Ind. Appl. (2025).

[15] Darshankumar Bhat, Stefan Muench, Mike Roellig, Estimation of remaining useful lifetime of power electronic components with machine learning based on mission profile data, Power Electron. Devices Components 5 (2023) 100040.

[16] Soroosh Alavi, Daniel Silva, Palash Pranav Vyas, Sa'd Hamasha, Evaluating the efficiency of machine learning approaches for predicting solder joint characteristic life under isothermal aging and thermal cycling test conditions, in: 2024 23rd IEEE Intersociety Conference on Thermal and Thermomechanical Phenomena in Electronic Systems, ITherm, IEEE, 2024, pp. 1–8.

[17] Jihen Rebai, Ahmed Ghorbel, Nabih Feki, Abdelkhalak El Hami, Mohamed Haddar, Supervised machine learning models for accurate prediction of CBGA solder joint lifespan, Mech. Adv. Mater. Struct. (2025) 1–20.

[18] S. Hochreiter, Long short-term memory, Neural Comput. MIT-Press (1997).

[19] Greg Van Houdt, Carlos Mosquera, Gonzalo Nápoles, A review on the long short-term memory model, Artif. Intell. Rev. 53 (8) (2020) 5929–5955.

[20] Ruiyang Zhang, Zhao Chen, Su Chen, Jingwei Zheng, Oral Büyüköztürk, Hao Sun, Deep long short-term memory networks for nonlinear structural seismic response prediction, Comput. Struct. 220 (2019) 55–68.

[21] Maziar Raissi, Paris Perdikaris, George E. Karniadakis, Physics-informed neural networks: A deep learning framework for solving forward and inverse problems involving nonlinear partial differential equations, J. Comput. Phys. 378 (2019) 686–707.

[22] Arunabha M. Roy, Suman Guha, A data-driven physics-constrained deep learning computational framework for solving von Mises plasticity, Eng. Appl. Artif. Intell. 122 (2023) 106049.

[23] A physics-informed deep learning framework for inversion and surrogate modeling in solid mechanics, Comput. Methods Appl. Mech. Engrg. 379 (2021) 113741.

[24] Mahdad Eghbalian, Mehdi Pouragha, Richard Wan, A physics-informed deep neural network for surrogate modeling in classical elasto-plasticity, Comput. Geotech. 159 (2023) 105472.

[25] Ruiyang Zhang, Yang Liu, Hao Sun, Physics-informed multi-LSTM networks for metamodeling of nonlinear structures, Comput. Methods Appl. Mech. Engrg. 369 (2020) 113226.

[26] Taniya Kapoor, Hongrui Wang, Alfredo Núnez, Rolf Dollevoet, Physics-informed neural networks for solving forward and inverse problems in complex beam systems, IEEE Trans. Neural Netw. Learn. Syst. 35 (5) (2024) 5981–5995.

[27] P.L. Wu, P.H. Wang, K.N. Chiang, Empirical solutions and reliability assessment of thermal induced creep failure for wafer level packaging, IEEE Trans. Device Mater. Reliab. 19 (1) (2018) 126–132.

[28] Ruiqian Zheng, Wenqian Li, Mengxuan Cheng, Hao Zheng, Zhiyan Zhao, Guoshun Wan, Yuxi Jia, Cross-scale finite element analysis of PCBA thermal cycling based on manufacturing history for more accurate fatigue life prediction of solder joints, Microelectron. Reliab. 160 (2024) 115473.

[29] Joshua A. Depiver, Sabuj Mallik, Emeka H. Amalu, Effect of creep, fatigue and random vibration on the integrity of solder joints in BGA package, Microelectron. Reliab. 157 (2024) 115415.

[30] C.Y. Tsou, T.N. Chang, K.C. Wu, P.L. Wu, K.N. Chiang, Reliability assessment using modified energy based model for WLCSP solder joints, in: 2017 International Conference on Electronics Packaging, ICEP, IEEE, 2017, pp. 7–15.

[31] COMSOL AB, COMSOL Multiphysics® v6.2, COMSOL AB, Stockholm, Sweden, 2023, Available at https://www.comsol.com.

[32] Robert Schwerz, René Metasch, Mike Roellig, Karsten Meier, FEM-study for solder model comparison on solder joints stress-strain effects, in: 2020 21st International Conference on Thermal, Mechanical and Multi-Physics Simulation and Experiments in Microelectronics and Microsystems, EuroSimE, IEEE, 2020, pp. 1–8.

[33] Shuai Zhang, Hongyun Zhao, Hongbo Xu, Xing Fu, Accelerative reliability tests for Sn3. 0Ag0. 5Cu solder joints under thermal cycling coupling with current stressing, Microelectron. Reliab. 120 (2021) 114094.

[34] Dania Bani Hani, Raed Al Athamneh, Mohammed Abueed, Sa'd Hamasha, Neural-fuzzy machine learning approach for the fatigue-creep reliability modeling of SAC305 solder joints, Sci. Rep. 13 (1) (2023) 8585.

[35] Qais Qasaimeh, Jia Liu, Daniel F Silva, Awni Qasaimeh, John L Evans, Sa'd Hamasha, Interpretable data-driven framework for life prediction of homogenous lead-free solder joints in ball grid array packages, J. Intell. Manuf. (2025) 1–19.

[36] Michael Osterman, Abhijit Dasgupta, Bongtae Han, A strain range based model for life assessment of Pb-free SAC solder interconnects, in: 56th Electronic Components and Technology Conference 2006, IEEE, 2006, pp. 7–pp.

[37] Ahmer Syed, Accumulated creep strain and energy density based thermal fatigue life prediction models for SnAgCu solder joints, in: 2004 Proceedings. 54th Electronic Components and Technology Conference (IEEE Cat. No. 04CH37546), Vol. 1, IEEE, 2004, pp. 737–746.

[38] Y.T. Su, K.N. Chiang, Using uncertainty analysis to validate reliability prediction in WLP with idealized solder joint modeling, in: 2024 19th International Microsystems, Packaging, Assembly and Circuits Technology Conference, IMPACT, IEEE, 2024, pp. 319–322.